Journal of Heat and Mass Transfer Research

Journal homepage: https://jhmtr.semnan.ac.ir

Semnan University

ISSN: 2383-3068

*Research Article*

# Experimental Study of Heat Transfer Augmentation Characteristics of a Tube Affected by Geometric Parameters of Coiled Spring Inserts

**Arvind Ashok Kapse *, Vinod Chimanrao Shewale**

*Department of Mechanical Engineering, M.V.P.S's K.B.T. College of Engineering, Nashik, 422013, Maharashtra, India*

**ARTICLE INFO**

***Article history:***

Received: 2023-03-05

Revised: 2024-01-31

Accepted: 2024-02-02

***Keywords:***

Passive insert;
Average performance ratio;
Turbulent flow

**ABSTRACT**

In the present study, the heat transfer and flow friction characteristics of a circular tube with coiled spring inserts are experimentally reported for a fully developed turbulent flow regime. Experimental investigations were performed in a circular concentric tube in a tube heat exchanger in the Reynolds number (Re) range of 8000–32,000 with water as a working fluid. The average Nusselt number ratio (Nua/Nup) and average friction factor ratio (fa/fp) with and without inserts are reported to be in the range of 1.79–2.79 and 2.44–4.17, respectively, for the tested six geometries of the inserts. The Nusselt number ratio (Nua/Nuc) based on equal pumping power criteria is also reported and found to be in the range of 0.94–1.24. The effects of varying pitch to length of insert ratio (p/l) and diameter of insert to the inner diameter of tube ratio (dc/Di) on heat transfer and pressure drop are reported, and empirical correlation is given for Nusselt number in terms of Reynolds number (Re), pitch to length of insert ratio (p/l), insert diameter to inner diameter of tube ratio (dc/Di), and Prandtl number (Pr).



## 1. Introduction

Many engineering applications typically use heat exchangers. Over the past few decades, numerous engineering techniques have emerged to enhance heat transfer within heat exchangers. Utilizing turbulator components to enhance fluid turbulence and, consequently, augment the heat transfer coefficient from the surface of the flow stands out among these methods. This approach has found extensive application across various heat exchanger uses, spanning refrigeration, automotive, process industries, and solar water heaters, among others. Its effectiveness lies in reducing heat exchanger dimensions while conserving energy. Broadly, heat transfer improvement methods fall into three categories: active, passive, and compound [1]. Active methods enhance heat transmission by employing external power sources. Passive methods involve incorporating turbulator elements inserted into tubes, while compound techniques combine both active and passive approaches. Previous researchers have extensively investigated heat transfer augmentation, and a collection of their work is presented here.

S. Eiamsa-ard et al. [2] experimentally compared, in the Reynolds number range of 4000 to 19000, the heat transmission and pressure loss of a single twisted tape and a dual twisted tape and recorded higher heat transfer rates for dual

* **Corresponding author.**
***E-mail address:*** *kapse.arvind@kbtcoe.org*

**Cite this article as:**

Kapse, A. A. and Shewale, V.C., 2024. Experimental Study of Heat Transfer Augmentation Characteristics of a Tube Affected by Geometric Parameters of Coiled Spring Inserts. *Journal of Heat and Mass Transfer Research*, 11(1), pp. 127-138.

https://doi.org/10.22075/JHMTR.2024.30106.1426

twisted tapes over single twisted tapes along with Nusselt number enhancement up to 146% and friction factor rise up to 256% over plain tube for a twist ratio (y/w) of 3.0 among three twist ratios of 3.0, 4.0, and 5.0 selected for study. This is attributed to the fact that the flow turbulence reduces for higher twist ratios due to a lesser number of turns. S. K. Singh and J. Sarkar [3] reported the thermo-hydraulic performance of a tapered wire coil turbulator in a double pipe heat exchanger using Al2O3 and MgO hybrid nanofluids for turbulent flow. It is seen that out of the three different configurations of coils tested, i.e., converging (C type), diverging (D type), and converging-diverging (C-D type), diverging (D type) wire coils give better thermo-hydraulic performance due to the higher contact surface area provided by the coil between fluid and tube wall surface when fluid decelerates from the D type wire coil. The authors reported the highest thermal performance factor of 1.69 for the D-type wire coil. K. Singh and J. Sarkar [4] studied the thermo-hydraulic performance of a conical wire coil enhancer of converging, diverging, and converging-diverging configurations using water-based mono (Al2O3 and CNT) and hybrid (Al2O3 + CNT) nanofluids. The authors reported the Nusselt number enhancements of 171%, 152%, and 139%, along with the friction factor increments of 106%, 92%, and 72%, respectively, for diverging, diverging-converging, and converging wire coil inserts compared to DI water in a plain tube. The heat transfer enhancement attributes to the weakened boundary layer are due to coils and swirl generated at different radial distances, along with increased thermal conductivity and flow turbulence caused by various slip mechanisms of nanoparticles. Moreover, the friction factor increments attribute to flow disturbance at the entry of the diverging coil.

Keklikcioglu and V. Ozceyhan [5] reported the influence of wire coils having convergent, convergent-divergent, and divergent shapes on heat transfer using ethylene glycol with water in three different mixture volumes (0:100), (20:80), and (40:60) as a working fluid in the Reynolds number range of 4627 to 25,099. It can be seen that both heat transfer and frictional resistance were increased for all wire coils. The addition of ethylene glycol to water reduced the heat transfer rate and increased the frictional resistance slightly. Garcia et al. [6] have experimentally validated a new methodology entitled TSP (Transition Shape Parameter), which enables the computation of the extension of the transitional flow region and the prediction of the evolution of the friction coefficient with wire-coil inserts. This methodology is a useful tool for choosing the best wire-coil design for a particular tubular heat exchanger because of the close relationship between the hydraulic and thermal performance of wire-coil inserts. M.E. Nakhchi et al. [7] employed the RNG k-ε model for numerical simulation to study the thermo-hydraulic behavior of perforated louvered strips in the Reynolds number range of 5000–14000. The results demonstrate that the recirculation flow through the holes of perforated louvered strips significantly improves the Nusselt number and thermal enhancement factor compared to louvered strips without holes. Better fluid mixing between the tube walls and core region is the main physical reason for heat transfer augmentation. Mehdi Bahiraei et al. [8] performed an experimental study to find the geometry effects of conical twisted strip inserts on the Nusselt number and the friction coefficient. The study noted that the Nusselt number and friction coefficient increased for all inserted cases and decreased with twist angle and pitch ratio due to the reduced turbulence caused by fewer turns at higher pitches. Also, a greater Nusselt number increment was observed at lower Reynolds numbers and diminished at higher Reynolds numbers, as the effect of flow turbulence is not significant in the turbulent regime. Subirana et al. [9] presented a numerical investigation of flow friction and heat transfer for a helical coil in a laminar and transitional regime, considering water as a working fluid. The authors investigated the interaction of the secondary swirl flow with the buoyancy motion and clarified the range where the heat transfer effect is worsened by the helical coil. Numerical results for the Nusselt number and friction factor were also validated with experimental results. R.M. Sarviya et al. [10] did experimental work to propose a new turbulator called a continuous cutting-edge helical lens insert. The experimental data on the Nusselt number and friction coefficient are collected from the new turbulator for two different swirl ratios of 3 and 5. Based on the results, the authors concluded that higher heat transfer rates can be achieved using twisted tape inserts with continuous cut edges at the expense of a reasonable pressure drop due to the flow separation augmented by the cutting edges of the insert.

Liu and Sakr [1] reviewed the experimental and numerical work of various researchers on passive augmentation techniques and mentioned that spiral ribbon inserts perform better for laminar flow than in turbulent flow. However, techniques such as conical rings, nozzles, etc., work better in turbulent flow. Kapse et al. [11] reviewed passive heat transfer augmentation techniques and highlighted their principles and thermo-hydraulic performance characteristics. Yang et al. [12] observed monotonical increments

in Nusselt number with Reynolds number and number of swirls in their investigation of convergent pipe fitted with a pre-swirl device at entry with air as a working medium between Reynolds numbers 7970 and 47820. Promvonge [13] investigated the effect of combining coils of wire and twisted ribbons in the Reynolds number range of 3000–18000 with air as the working medium and found that the use of combined turbulators is more effective at low Reynolds numbers due to two different mechanisms of weak boundary layer by wire coil and swirl induced by twisted ribbons. Sumit Kumar Singh and Jahar Sarkar [14] experimentally compared the performance of V-cut twisted tapes and tapered wire coils using Al2O3+MWCNT hybrid nanofluid in the Reynolds number range of 8000–40000 for a volume concentration of 0.01%. The investigation reported a higher heat transfer coefficient for tapered wire coils compared to V-cut twisted tapes due to a weak boundary layer supported by swirls induced at different radii in the tube. Based on PEC and FOM criteria, V-cut twisted tapes provided an advantage over wire coils due to lesser pressure drop augmentation.

It can be concluded from the reviewed literature that coiled wire inserts do not cause sudden pressure drops or higher heat transfer enhancement. Due to their helical shape, the coiled wires introduce swirls in the flow, resulting in better heat transfer rates. Furthermore, it is noteworthy that the coil wires are less tested individually in turbulent flow regimes for various geometric parameters like coil diameter, pitch, wire size, etc. In the present investigation, the experimental results of heat transfer and flow friction of coiled spring inserts of varying geometries are reported in the turbulent flow regime. Six geometries have been prepared for two varying parameters, i.e., the coil diameter and the pitch of the coil.

## 2. Experimental Setup and Methodologies

### *2.1. Coiled Spring Insert Details:*

A coiled spring insert is prepared manually by wounding the selected wire of 0.8 mm diameter over a rod of suitable diameter to maintain the required size of the coiled spring. The pitch-to-length of the coiled spring ratio (p/l) and coiled spring diameter to the inner tube diameter ratio (dc/Di) are varied, and six configuration geometries have been prepared for full-length insertion as shown in Table 1, and a sample picture of the coiled spring insert is shown in Fig. 1.

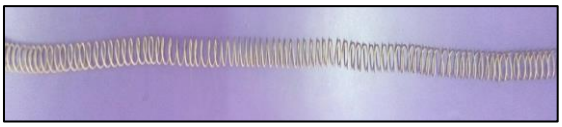

**Fig. 1.** Actual picture of coiled spring insert

**Table 1.** Details of the configuration geometries of coiled spring insert

| Configuration No. | Diameter of coil (mm) | Pitch of coil (mm) | dc/Di Ratio | p/l Ratio |
|---|---|---|---|---|
| 1 | 18.2 | 5 | 0.85 | 0.000625 |
| 2 | 18.2 | 10 | 0.85 | 0.00125 |
| 3 | 18.2 | 15 | 0.85 | 0.001875 |
| 4 | 15.6 | 5 | 0.728 | 0.000625 |
| 5 | 15.6 | 10 | 0.728 | 0.00125 |
| 6 | 15.6 | 15 | 0.728 | 0.001875 |

### *2.2. Arrangement of Experimental Setup*

The arrangement of the experimental set is shown in Fig. 2.

Before the trials with inserts are conducted, plain tube results are required to be validated with well-established equations to gain confidence in the experimental work. Hence, the trials are conducted initially on plain tubes for validation of the experimental setup between the Reynolds number ranges of 8000 and 32000, with the Reynolds number increasing by a step of 4000. After plain tube validation, trials are conducted for inserted tube cases. The following procedure is followed for conducting trials:

The water stored in a 100-liter hot water tank equipped with five 2 kW heaters is heated to a temperature of 75°C and then circulated through the ring in a closed circuit with a hot water circulation pump. The hot water tank is deliberately kept 0.5 m above the hot water circulation pump to avoid the possibility of cavitation. A shut-off valve installed in the hot water circulation pipe maintains the necessary flow rate. The flow rate is calculated from the differential manometer reading of the U-tube manometer connected to a pre-calibrated Venturi meter. After that, cold water is fed counter-currently from a large underground water tank through an inner tube (test section) through a cold water circulation pump in a closed circuit. The required flow rate is maintained in the cold water circulation line by one bypass valve and two shut-off valves. The cold water flow rate is calculated by measuring the differential pressure head with a manometer through a calibrated venturi meter located in the cold water piping upstream of the test section. The pressure drop in the test section is measured by a U-tube manometer, whose manometric liquid is carbon tetrachloride (CCL4).

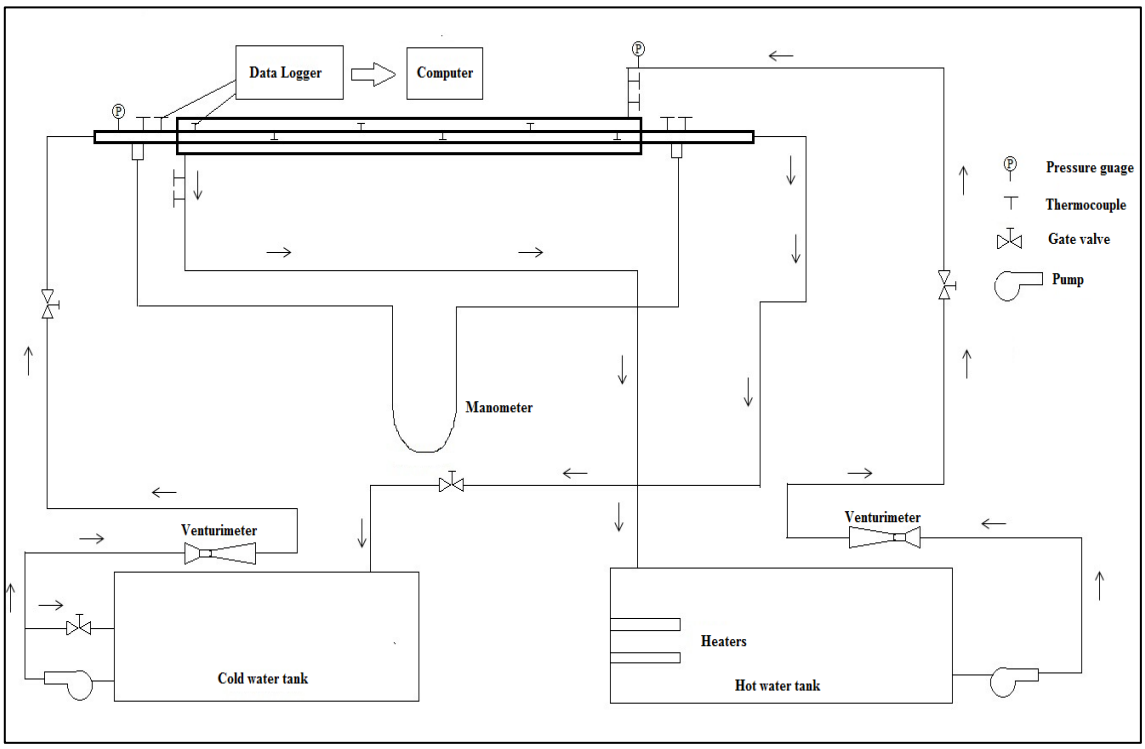


**Fig. 2.** Arrangement of experimental setup [15]

The system is then allowed to reach a steady state, and temperatures and pressure drops are measured for a plain tube at a cold water Reynolds number based on the test section inlet of 8000–32000.

All required temperatures are measured using pre-calibrated copper/constantan T-type thermocouples connected to the data acquisition system. Cold and hot water temperatures are measured at the inlet and outlet points of the test section with two thermocouples placed at each location, and the average temperature is measured to improve accuracy. The outer surface wall temperature of the tube test section is measured by six thermocouples, which are placed around and equidistant from the surface. The details of the experimental setup and test conditions are shown in Table 2, and a complete photo of the experimental setup is shown in Fig. 3.

**Fig. 3.** A photograph of actual setup

**Table 2.** Details of experimental setup and test conditions

| | | |
|---|---|---|
| **A)** | **Experimental setup** | |
| 1. | Type of Heat Exchanger | Tube in tube heat exchanger |
| 2. | Inner tube inner diameter | 21.4mm |
| 3. | Inner tube thickness | 3.65 mm |
| 4. | Outer tube inner diameter | 48.3mm |
| 5. | Outer tube thickness | 5.85mm |
| 6. | Length of test section | For heat transfer 0.8m, For pressure drop |
| 7. | Manometric fluid | Carbon Tetrachloride, $CCL_4$(density 1577 kgkg/m$^3$) |
| 8. | Pressure measurement | U tube manometer (uncertainty ±1mm of |
| 9. | Flow measurement | Venturimeter (uncertainty ±0.0125 kg/sec) |
| 10. | Temperature measurement | T type thermocouple (uncertainty ±0.4°C) |
| **B)** | **Test conditions** | |
| 1. | Cold water inlet temperature | 25 °C |
| 2. | Hot water inlet temperature | 75°C |
| 3. | Range of Reynolds number, ($Re$) | 8000 to 32000 |

### 2.3. Validation of Test Setup

Based on the test data collected from the standard test tube tests, the test setup is validated as described in the next section.

#### 2.3.1. Plain Tube Validation

The experimental values of Nusselt number and friction coefficient for a standard circular pipe are compared with the following established equations:

$$Nu = 0.023Re_p^{0.8}Pr^{0.4} \quad \text{(Dittus Boelter)} \quad (1)$$

$$Nu = \frac{(f/8)(Re-1000)Pr}{1+12.7(f/8)^{1/2}(Pr^{2/3}-1)} \quad \text{(Gnielinski)} \quad (2)$$

$$f = 0.079Re^{-0.25} \quad \text{(Blasius)} \quad (3)$$

**Table 3.** Uncertainties in the measurements

| Sr. No. | Parameter | Uncertainty |
|---|---|---|
| 1. | Pressure | ±1 mm of $CCL_4$ column |
| 2. | Flow | ±0.0125 kg/sec |
| 3. | Temperature | ±0.4 ˚C |
| 4. | Reynolds number (Re) | ±6.54% |
| 5. | Augmented tube Nusselt number (Nua) | ±8.85% |
| 6. | Equivalent Nusselt number (Nuc) | ±10.82% |
| 7. | Friction factor | ±12.67 % |

A comparison of the experimental results of Nusselt number and friction coefficient with the above equations is shown in Figures 4 and 5.

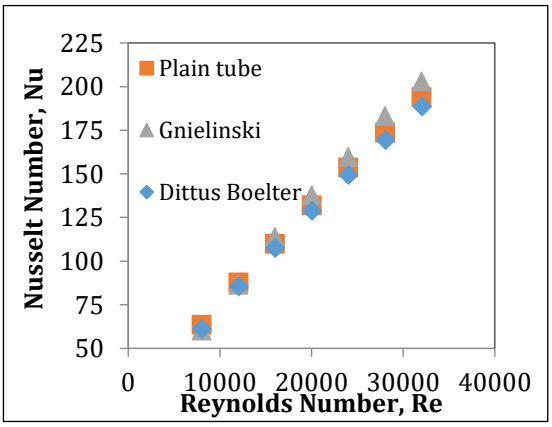


**Fig. 4.** Nusselt number for plain tube [16]

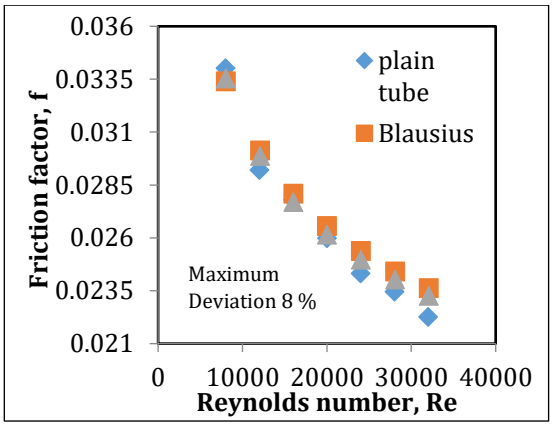


**Fig. 5.** Friction factor for plain tube [16]

It can be seen from the figures that the experimental results agree well with the above equations within 10% of the Nusselt number and 8% of the friction coefficient. Thus, plain -tubes are verified, and further test runs are conducted for coiled spring inserts.

#### 2.3.2. Inserted Ttube Validation

As new geometries are proposed in the experiment, the Nusselt number and friction coefficients of the embedded tube are confirmed by testing the same geometries used by previous researchers. Experimental results are compared with the data from two research papers for heating and cooling the test section.

##### 2.3.2.1. Heating of the Test Section

Jian Guo et al. [17] have tested different geometries of conical strip inserts in their work for heating the test section, with water being a working fluid between the Reynolds numbers of 5000 and 25000. The present experimental results are compared with this available data between the Reynolds numbers of 8000 to 23000 within a step of 3000, as shown in figs. 6 and 7.

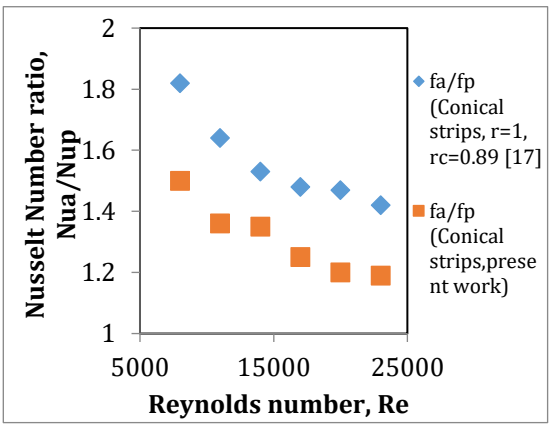


**Fig. 6.** Nusselt number ratios for inserted tube (Heating)

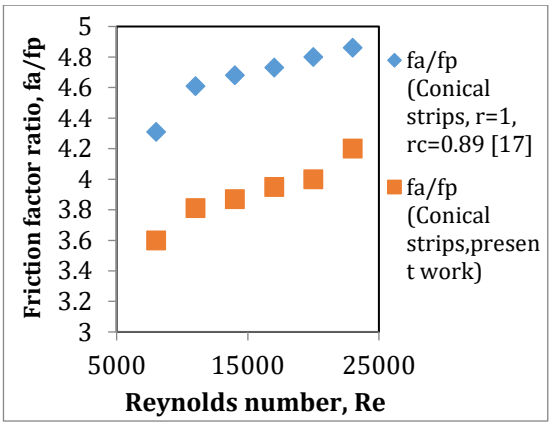


**Fig. 7.** Friction factor ratios for inserted tube (Heating)

The experimental results match the available data, with an accuracy of ± 22% for the Nusselt number and 21% for the friction coefficient.

*2.3.2.2. Cooling of the Test Section*

Promvonge et al. [18] have tested louvered strip inserts for cooling the test section in the Reynolds number range of 6000 to 42000. The present experimental results for one of the geometries (backward arrangement inclined angle 25˚) are compared with this available data in the Reynolds number range of 8000 to 32000 within a step of 4000 as shown in figs. 8 and 9.

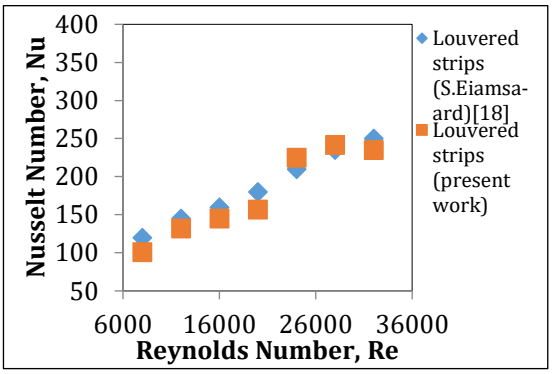


**Fig. 8.** Nusselt number for inserted tube (Cooling)

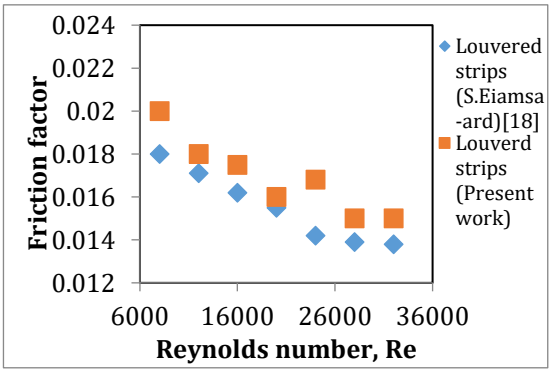


**Fig. 9.** Friction factor for inserted tube (Cooling)

Experimental results agree well within ± 18% for the Nusselt number and 16% for the friction factor. The above deviations might be caused by manufacturing errors involved during the preparation of the inserts, as per the details given in the papers.

## 3. Analysis of Data

The experimental data collected for temperatures, pressure, and mass flow rates is analyzed as follows for the evaluation of the performances of selected inserts.

The average Nusselt number and the friction coefficient are calculated from the inside diameter of the test piece as follows:

The thermal gain of cold water is obtained as follows:

$$Q_c = \dot{m}_c C_{p,w}(T_{c,out} - T_{c,in}) \quad (4)$$

The thermal loss of hot water in annulus is calculated as:

$$Q_h = \dot{m}_h C_{p,w}(T_{h,in} - T_{h,out}) \quad (5)$$

Due to convection and radiation losses, the difference in heat gain between cold water and hot water was found to be 3-10%. Thus, the average inner heat transfer coefficient (hi) is calculated based on the average heat transfer rate ($Q_{avg}$)

$$Q_{avg} = \frac{Q_c + Q_h}{2} \quad (6)$$

When calculating the average heat transfer coefficient of the inner side, it is assumed that the surface temperature of the tube wall is constant. Therefore, neglecting the thermal resistance of the copper pipe wall, the heat transfer coefficient (hi) is calculated as follows [19]:

$$Q_{avg} = h_i A_i \Delta T_{lm} \quad (7)$$

where

$$\Delta T_{lm} = \frac{(\tilde{T}_s - T_{c,out}) - (\tilde{T}_s - T_{c,in})}{\ln[(\tilde{T}_s - T_{c,out})/(\tilde{T}_s - T_{c,in})]} \quad (8)$$

And

$$A_i = \pi D_{i,} L \quad (9)$$

The surface temperature of the tube wall is considered to be the average temperature of the temperatures recorded by six thermocouples (test section) placed on the outer surface of the tube wall. ($\tilde{T}_s$)

$$\tilde{T}_s = \sum T_s/6 \quad (10)$$

The average Nusselt number is obtained from the average heat transfer coefficient as:

$$Nu = \frac{h_i D_h}{k} \quad (11)$$

The average friction factor coefficient is calculated as follows:

$$f = \frac{\Delta P}{\left(\frac{L1}{D_i}\right)\left(\rho\frac{V^2}{2}\right)} \quad (12$$

where V is the average velocity of the working fluid in the inner tube. Thermophysical properties are measured at bulk mean average temperature of the liquid.

### *3.1. Performance Evaluation Criteria [20]*

The performance evaluation criteria for enhancement techniques are decided based on the following performance objectives:

Reduced heat transfer surface material for fixed heat duty and pressure drop, reduced LMTD for fixed heat duty and surface area, increased heat duty for a fixed surface area, reduced pumping power requirements for fixed heat duty and exchanger surface area.

Bergles et al. [20] suggested a set of eight numbers of performance evaluation criteria to achieve these objectives. Performance evaluation criteria have been used for the present experimental work to determine heat transfer enhancement for coiled spring inserts. Corresponds to the ratio of the augmented tube Nusselt number to the plain tube Nusselt number at the same Reynolds number, while the term The average performance ratio (APR) is the ratio of the Nusselt number of the inserted tube to the Nusselt number of the plain tube, corresponding to equal pumping power as it is required for the inserted tube to maintain the flow. The performance ratio is derived as follows [21]:

Assuming,

$Nu_a$ = Nusselt number of tube with augmentation

$Nu_p$ = Nusselt number of plain tube

$Nu_c$ = Nusselt number of plain tube at equivalent pumping power as required by tube with augmentation

Similarly $f_a$, $f_p$, $f_c$ are the friction factors of above cases respectively.

For any flow through pipe having volume flow rate $\dot{Q}$ and frictional pressure drop ΔP, the pumping power is given by:

$$\text{Pumping power} = \Delta P \times \dot{Q} \quad (13)$$

$$= \left(\frac{4fLV^2}{2gD}\right) \times \rho g \times AV \quad (14)$$

where A is the cross sectional area of pipe and V is the mean fluid velocity in m/sec.

Thus

Pumping power = $fV^3$

i.e. Pumping power $\propto fV^3$

Reynolds number Re is given by

$$Re = \frac{\rho VD}{\mu} \quad (15)$$

$$\therefore Re \propto V$$

$$\therefore \text{Pumping power} \propto (f\,Re^3)$$

Thus for equal pumping power

$$f_a \times {Re_a}^3 = f_p \times {Re_c}^3 \quad (16)$$

For plain tube, frictional factor by Blausius is given by

$$f_p = \frac{0.079}{{Re_c}^{0.25}} \quad (17)$$

Putting in equation (16). The equivalent Reynolds number is given by

$$Re_c^{2.75} = f_a \times \frac{Re_a^3}{0.079} \quad (18)$$

The Nusselt number for equivalent plain tube Reynolds number $Re_c$ is calculated from Dittus Boelter Equation as follows:

$$Nu_c = 0.023 Re_c^{0.8} Pr^{0.4} \quad (19)$$

The average performance ratio is calculated as follows:

$$R_3 = \frac{Nu_a}{Nu_c} \quad (20)$$

## 4. Results and Discussion

### *4.1. Effect of Insert on Thermo Hydraulic Performance*

The effect of a coiled spring insert on heat transfer is shown in terms of Nusselt number enhancement in figs. 10 and 11. Results reveal that the coiled spring insert gives enhanced heat transfer rates in comparison to the plain tube for all selected geometries of the insert. The Nusselt number enhancement of the inserted tube is reported in the range of 1.08 to 1.55 over a plain tube. This can be attributed to the swirls and vortices created in the flow due to the spiral shape of the coiled spring. The increased swirl and vortices created would result in thinning the boundary layer, causing higher heat transfer rates.

It can be observed from Figs. 10 and 11 that the Nusselt number ratio (Nua/Nup) tends to decrease with increasing Reynolds numbers, diminishing the heat transfer enhancements. This can be attributed to the fact that the effect of turbulent flow on heat transfer increases in turbulent flow regimes.

The average friction factor ratios for the insert are shown in Figs. 12 and 13. Due to the higher fluid inertia in the plain tube and augmented tube cases, it is seen that the friction factor decreases with increasing Reynolds numbers. As a result, the average friction factor ratio stays almost constant at varying Reynolds numbers.

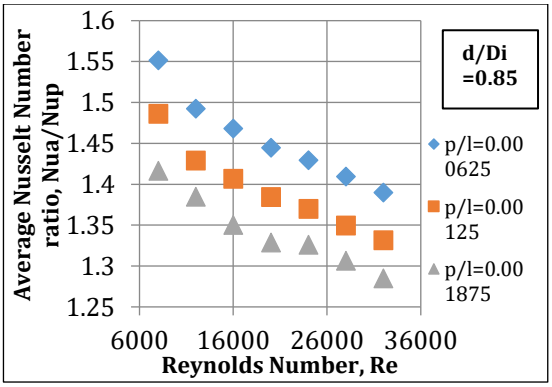


**Fig. 10.** Average Nusselt Number Ratio Vs Reynolds Number

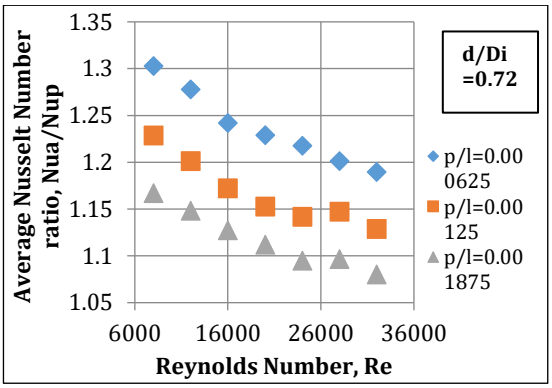


**Fig. 11.** Average Nusselt Number Ratio Vs Reynolds Number

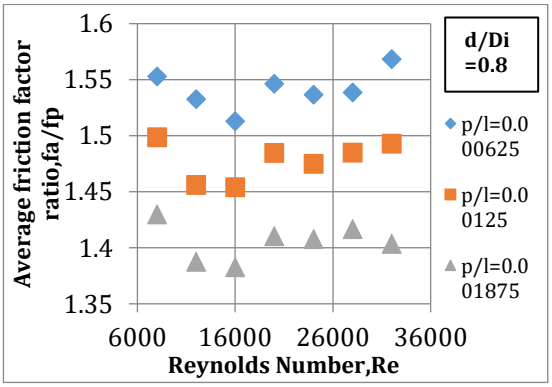


**Fig. 12.** Average Friction Factor Ratio Vs Reynolds Number

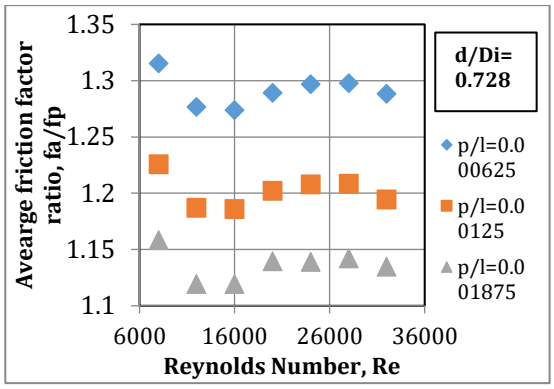


**Fig. 13.** Average Friction Factor Ratio Vs Reynolds Number

### *4.2. Effect of [dc/Di] and [p/l] Ratio*

It can be seen from Figs. 10 and 11, the heat transfer enhancement is affected by the pitch-to-length of the insert ratio (p/l). The average Nusselt number ratio increases from 1.167 at p/l = 0.001875 to 1.55 at p/l = 0.000625 for a Reynolds number of 8000. The corresponding values reported for Reynolds number 32000 are 1.08 to 1.38. These results reveal that heat transfer is enhanced by decreasing p/l ratios. This can be attributed to the increased surface contact area of the fluid due to the increased number of turns completed, which causes a higher swirl in the flow. Higher p/l ratios cause the flow to complete fewer spins, which reduces the swirl and the surface area of fluid in contact with the inner tube wall. As a result, there would be a decrease in the laminar sublayer breaking effect and heat transfer rates.

The heat transfer enhancement is also affected by the dc/Di ratio, as shown in Figs. 10 and 11. It is seen that the average Nusselt number ratio reduces from 1.55 for dc/Di = 0.85 to 1.3 for dc/Di = 0.728 at a Reynolds number of 32000 for a constant p/l ratio of 0.000625. The boundary layer would be thinner for a higher dc/Di ratio (higher coil diameter) due to the increased surface contact of the coil with the tube wall touching the maximum fluid mass. However, for lower dc/Di ratios (lower coil diameter), a gap between the tool and tube wall would be increased, resulting in a thicker boundary layer near the tube wall and reduced heat transfer rates.

The influence of p/l and dc/Di ratios on friction factor is presented in Figs. 12 and 13. The observation reveals a decrease in the friction factor as the p/l ratio increases because a greater pitch reduces the contact surface area between the coil and the fluid. Moreover, with larger coil diameters, the dc/Di ratio increases, leading to greater obstruction of the flow area and consequently causing a higher pressure drop. At a Reynolds number of 8000, the insert with a p/l ratio of 0.000625 and a d/Di ratio of 0.85 exhibits

the highest observed friction factor ratio, fa/fp. Conversely, at a Reynolds number of 32,000, the insert with ratios p/l = 0.001875 and d/Di = 0.728 displays the lowest observed friction factor ratio, fa/fp. The friction factor declines as the Reynolds number increases because of the heightened momentum within the fluid. However, it can be observed that the ratio of friction factors fa/fp appears to stabilize at higher Reynolds numbers, remaining nearly constant.

The experimental results of the Nusselt number for the tube with coiled spring inserts are correlated depending on the (p/l) and (dc/Di) ratios as follows:

$$Nu = 0.05Re^{0.71}Pr^{0.35}(dc/Di)^{0.22}(p/l)^{-0.09} \quad (21)$$

The experimental Nusselt number and predicted Nusselt number by equation 21 are compared in Fig. 14. A maximum deviation of 19.8% is observed between the experimental Nusselt number and the predicted Nusselt number in equation 21.

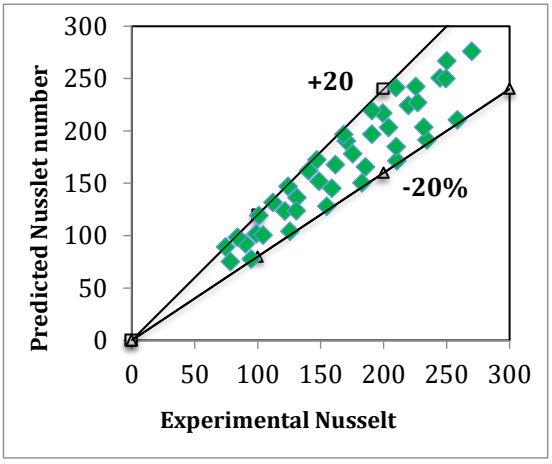


**Fig. 14.** A Comparison of experimental and predicted Nusselt number

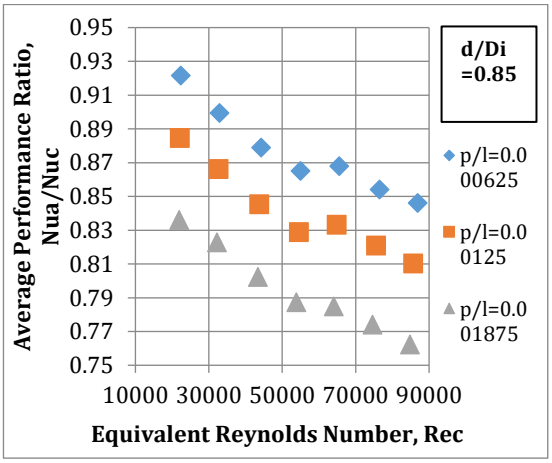


**Fig. 15.** Average Performance Ratio Vs Equivalent Reynolds Number

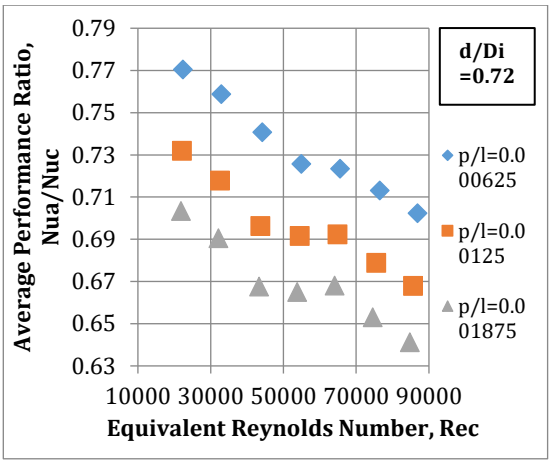


**Fig. 16.** Average Performance Ratio Vs Equivalent Reynolds Number

The average Nusselt numbers for plain tubes, which equate to the pumping power necessary to overcome the flow friction caused by inserts, are computed in relation to the performance ratio, R3 (Nua/Nuc), and are presented in Figs. 15 and 16.

As shown in the figures, a decreasing trend of the average performance ratio with increasing Reynolds number is seen across all coil geometries. The trend observed indicates that the average performance ratio diminishes as the p/l ratio increases and the dc/Di ratio decreases. Furthermore, it is noted that for nearly all the cases examined, the average performance ratio R3 (Nua/Nuc) remains less than unity. Thus, due to the penalty in the form of additional pumping power required to maintain the flow, the net gain in terms of energy savings is negative for all the examined coil geometries. The maximum average performance ratio is obtained for the insert with p/l = 0.000625, and d/Di = 0.85 at Reynolds number 8000, and the minimum average performance ratio is obtained for the insert with p/l = 0.001875 and d/Di = 0.728 at Reynolds number 32,000. Looking into the increased pumping power requirements and range of performance ratios observed, the thermohydraulic performance of the insert is not competitive in the selected range of Reynolds numbers.

## 5. Conclusions

The effects of geometric parameters of the coiled spring on thermohydraulic performance are evaluated for turbulent flow in the Reynolds number range of 8000–32000. The average Nusselt number enhancement was reported to be in the range of 8% to 55.12% for selected geometries of the inserts, along with the friction factor enhancement between 11.93% and 56.82%. It is seen that both the geometric parameters, i.e., coil diameter to inner tube diameter (dc/Di) and pitch to length of insert

ratio (p/l), affect the thermo-hydraulic performance of the insert. Due to increased swirl and contact area at higher (dc/Di) and lower (p/l), the heat transfer performance was improved. The maximum average Nusselt number ratio at equal pumping power (Nua/Nuc) was reported for coils with (dc/Di) = 0.85 and (p/l) = 0.000625. This reveals that the coiled spring inserts are suitable for heat transfer augmentation in applications where pumping power requirements are of minor concern.

## Nomenclature

A Area, [$m^2$]

dc Spring Coil Diameter [m]

$Di$ Tube Inner Diameter, [m]

$p$ Pitch of the spring coil [m]

$l$ Length of insert [m]

$\Delta P$ Pressure drop of fluid, [$Nm^{-2}$]

$T_{lm}$ Logarithmic mean temperature difference, [°C]

$H$ Heat transfer coefficient,[$Wm^{-2}K^{-1}$]

$K$ Thermal conductivity, [$Wm^{-1}K^{-1}$]

$L$ Length of insert, [m]

$L$ Length of test section for heat transfer, [m]

$L_1$ Length of tube between pressure taps, [m]

$r$ Dimensionless length of the conical strip

$r_c$ Dimensionless radius of core-cutting

$\dot{m}$ Mass flow rate of fluid, [$kgsec^{-1}$]

$Q$ Heat transfer rate, [kW]

$T$ Temperature, [°C]

$V$ Mean fluid velocity, [$msec^{-1}$]

$C_{P,W}$ Specific heat at constant pressure, [$kJkg^{-1}K^{-1}$]

$Re$ Reynolds number (=$\rho VD/\mu$), [-]

$R3$ Average performance ratio, [-]

$Pr$ Prandtl number (=$\mu C_p/k$), [-]

$f$ Average friction factor, [-]

$Nu$ Average Nusselt number, [-]

*Greek symbols*

$\rho$ Density of fluid, [$kgm^{-3}$]

$\mu$ Dynamic viscosity, [$kgms^{-1}$]

*Subscripts*

$a$ Augmented tube case

$avg$ Average

$c$ Cold

$h$ Hot

$i$ Inner

$in$ Inlet

$o$ Outer

$out$ Outlet

$p$ Plain tube case

$s$ Tube wall surface

## Acknowledgments

The authors would like to express their gratitude to Dr. S. V. Kasar and Dr. P. W. Deshmukh for providing insight and expertise that contributed greatly to the research. The authors would also like to thank Dr. S. B. Sonawane for comments that greatly improved the manuscript.

## Funding Statement

This research did not receive any specific grant from funding agencies in the public, commercial, or not-for-profit sectors.

## Conflicts of Interest

The author declares that there is no conflict of interest regarding the publication of this article.

## References

[1] Liu, S., & Sakr, M., 2013. A comprehensive review on passive heat transfer enhancements in pipe exchangers. Renewable and sustainable energy reviews, 19, pp. 64-81.

[2] Eiamsa-Ard, S., Thianpong, C., Eiamsa-Ard, P. and Promvonge, P., 2010. Thermal characteristics in a heat exchanger tube fitted with dual twisted tape elements in tandem. International Communications in Heat and Mass Transfer, 37(1), pp. 39-46.

[3] Singh, S. K., & Sarkar, J., 2020. Improving hydrothermal performance of hybrid nanofluid in double tube heat exchanger using tapered wire coil turbulator. Advanced Powder Technology, 31(5), pp. 2092-2100.

[4] Singh, S. K., & Sarkar, J., 2021. Thermohydraulic behavior of concentric tube heat exchanger inserted with conical wire coil using mono/hybrid nanofluids. International Communications in Heat and Mass Transfer, 122, p. 105134.

[5] Keklikcioglu, O., & Ozceyhan, V., 2022. Heat transfer augmentation in a tube with conical wire coils using a mixture of ethylene glycol/water as a fluid. International Journal of Thermal Sciences, 171, p. 107204.

[6] García, A., Herrero-Martin, R., Pérez-García, J., & Solano, J. P., 2023. Validation of a new methodological approach for the selection of wire-coil inserts in thermal equipment. Applied Thermal Engineering, 218, p. 119273.

[7] Nakhchi, M. E., Esfahani, J. A., & Kim, K. C., 2020. Numerical study of turbulent flow inside heat exchangers using perforated louvered strip inserts. International Journal of Heat and Mass Transfer, 148, p. 119143.

[8] Bahiraei, M., Gharagozloo, K., & Moayedi, H. 2020. Experimental study on effect of employing twisted conical strip inserts on thermohydraulic performance considering geometrical parameters. International Journal of Thermal Sciences, 149, p. 106178.

[9] Subirana, A.M., Solano, J.P., Herrero-Martín, R., García, A. and Pérez-García, J., 2023. Mixed convection phenomena in tubes with wire coil inserts. Thermal Science and Engineering Progress, 42, p. 101839.

[10] Sarviya, R. M., & Fuskele, V., 2018. Heat transfer and pressure drop in a circular tube fitted with twisted tape insert having continuous cut edges. Journal of Energy Storage, 19, pp. 10-14.

[11] Kapse, A. A., Shewale, V.C., Mogal, S. P., and Kakade, A B., 2023. A comprehensive review on passive heat transfer enhancements in pipe exchangers. JP journal of heat and mass transfer, 35, pp. 153-185.

[12] Yang, C. S., Jeng, D. Z., Yang, Y. J., Chen, H. R., & Gau, C., 2011. Experimental study of pre-swirl flow effect on the heat transfer process in the entry region of a convergent pipe. Experimental Thermal and Fluid Science, 35(1), pp. 73-81.

[13] Promvonge, P., 2008. Thermal augmentation in circular tube with twisted tape and wire coil turbulators. Energy Conversion and Management, 49(11), pp. 2949-2955.

[14] Singh, S. K., & Sarkar, J., 2021. Hydrothermal performance comparison of modified twisted tapes and wire coils in tubular heat exchanger using hybrid nanofluid. International Journal of Thermal Sciences, 166, p. 106990.

[15] Kapse, A. A., Dongarwar P. R., and Gawande, R. R., 2017. Thermo hydraulic Performance Comparison of Compound Inserts. Thermal Science, 21, pp. 1309-1319

[16] Kapse, A. A., Dongarwar, P. R., & Gawande, R. R., 2017. Experimental investigation of turbulent heat transfer performance in internal flow using a star shape cross sectioned twisted rod inserts. Heat and Mass Transfer, 53, pp. 253-264.

[17] Guo, J., Yan, Y., Liu, W., Jiang, F., & Fan, A. 2013. Effects of upwind area of tube inserts on heat transfer and flow resistance characteristics of turbulent flow. Experimental thermal and fluid science, 48, pp. 147-155.

[18] Eiamsa-ard, S., Pethkool, S., Thianpong, C., & Promvonge, P. 2008. Turbulent flow heat transfer and pressure loss in a double pipe heat exchanger with louvered strip inserts. International Communications in Heat and Mass Transfer, 35(2), pp. 120-129.

[19] Incropera, F.P., and DeWitt, D.P., 2010. Fundamentals of Heat and Mass Transfer, Wiley.

[20] Bergles, A.E., Blumenkrantz, A.R., and Taborek, J., 1974. Performance evaluation criteria for enhanced heat transfer surfaces. In International Heat Transfer Conference 5 (IHTC-5), Tokyo, Japan, pp. 239-243. DOI: 10.1615/IHTC5.2130.

[21] Deshmukh, P. W., & Vedula, R. P., 2014. Heat transfer and friction factor characteristics of turbulent flow through a circular tube fitted with vortex generator inserts. International Journal of Heat and Mass Transfer, 79, pp. 551-560.